

Infrastructure Change Monitoring Using Multitemporal Multispectral Satellite Images

U. Datta

Abstract—The main objective of this study is to find a suitable approach to monitor the land infrastructure growth over a period of time using multispectral satellite images. Bi-temporal change detection method is unable to indicate the continuous change occurring over a long period of time. To achieve this objective, the approach used here estimates a statistical model from series of multispectral image data over a long period of time, assuming there is no considerable change during that time period and then compare it with the multispectral image data obtained at a later time. The change is estimated pixel-wise. Statistical composite hypothesis technique is used for estimating pixel based change detection in a defined region. The generalized likelihood ratio test (GLRT) is used to detect the changed pixel from probabilistic estimated model of the corresponding pixel. The changed pixel is detected assuming that the images have been co-registered prior to estimation. To minimize error due to co-registration, 8-neighborhood pixels around the pixel under test are also considered. The multispectral images from Sentinel-2 and Landsat-8 from 2015 to 2018 are used for this purpose. There are different challenges in this method. First and foremost challenge is to get quite a large number of datasets for multivariate distribution modelling. A large number of images are always discarded due to cloud coverage. Due to imperfect modelling there will be high probability of false alarm. Overall conclusion that can be drawn from this work is that the probabilistic method described in this paper has given some promising results, which need to be pursued further.

Keywords—Co-registration, GLRT, infrastructure growth, multispectral, multitemporal, pixel-based change detection.

I. INTRODUCTION

THE main objective of the study is to identify a suitable approach for monitoring the various types of infrastructure growth on land occurring over a time period. Interesting infrastructure growth phenomena are artificial surfaces i.e. built-up land, rail network construction, road construction in and near airport and harbor. The case study in this report is the infrastructure growth over a period of time near harbor area.

The change detection in remote sensing is the process of identifying differences in the state of an object or a phenomenon by observing it at different time instants [1], [2]. The technique of change detection for remote sensing data has been developed with increase in the spatial resolution of remote sensing images [3]. The change is due to variation in reflectance data [4] from the scene. Even if the images with no change in the scene are taken from same satellites, the change can be due to different reasons like images taken at different

time of the day, taken at different seasons, taken from different angles etc. The co-registration accuracy also affects the change detection, especially in the case of pixel-wise change detection [5]. In this case the interest is to monitor the infrastructural growth, which is mostly due to change in material property. It is not an easy task to identify such changes due to variation of material nature or material change. Literature survey shows various known methods used for change detection [6], which include image overlay, image differencing, image regression, image rationing, vegetation index differencing, post-classification comparison, principal components analysis, spectral/temporal classification, change vector analysis, background subtraction etc.

Most of the change detection methods are bi-temporal i.e. comparing the images of the same scene taken at two different times from same remote sensing source. In most of the cases this type of work is done using images of single modality. Literature survey [7] indicates that some work is done using dual modality especially using high spatial resolution optical and synthetic aperture radar data. Our main objective is to monitor the infrastructure growth over a period of time. To achieve this type of objective the approach used here is to estimate a statistical model from series of multispectral image data over a long period of time assuming no considerable change occurred and then compare it with the multispectral image data obtained at a later time. The probabilistic approach is perhaps the best suitable technique for this type of processing. Main motivation of this approach is to use an existing probabilistic approach used in hyperspectral images [7] to identify the anomaly from clutter or background and assess to what extent this method is applicable for this infrastructure change monitoring. The composite hypothesis theory is a well-established binary method for target detection or anomaly detection. It is considered to estimate the model pixel-wise and then identify the changed pixel at a later time instant. In this paper the multispectral data sets from remote sensing satellites Sentinel-2 MSI (Multispectral Instrument) and Landsat-8 are used to validate the model.

II. DATASET AND PREPROCESSING

For this study, Sentinel-2 as well as Landsat-8 datasets from the area called Stockholm Norvik Hamn are downloaded. Fig. 1 is showing the region selected for analysis. It is Sweden's harbor area. In this area, there is an ongoing project for building the harbor for rolling goods and containers at Norvikudden, outside Nynashamn. In addition to the harbor, a railway is also being connected to Nynas railway network, and a construction group is building a logistics and business park

U. Datta is Scientist at the Norwegian Defence Research Establishment (FFI), Instituttvn 20, Kjeller 2007, and Norway (phone: 0047-915-030003; e-mail: uda@ffi.no).

adjacent to the harbor. In Fig. 1 (a) is taken in 2015 and (b) in 2018. Visual inspection shows the change due to infrastructure growth. So in first thought, it is a right choice of area for our preliminary analysis.

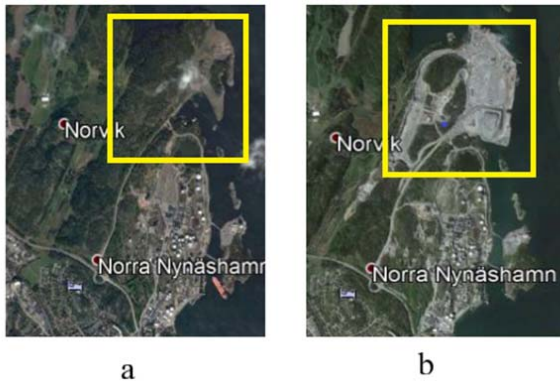


Fig. 1 The picture of Stockholm Norvik Hamn taken from Google earth. (a) is taken in 2015 and (b) is taken in 2018

TABLE I
SPATIAL RESOLUTION (M) AND SPECTRAL RANGE (NM) OF SENTINEL-2 MSI

Band Number	Spatial Resolution in m	Spectral Range in nm
B1	60	443±10
B2	10	490±32.5
B3	10	560±17.5
B4	10	665±15
B5	20	705±7.5
B6	20	740±7.5
B7	20	783±10
B8	10	842±57.5
B8A	20	865±10
B9	60	945±10
B10	60	1375±15
B11	20	1610±45
B12	20	2190±90

The Copernicus Open Access Hub provides complete, free and open access to Sentinel-2 user products. Table I shows the list of spectral bands available for multivariate analysis of Sentinel-2 images. The Landsat products are also available at free of cost to the user for download at Earth Explorer. Table II shows list of bands available for Landsat-8. The data are searched in chosen area for a particular time interval and downloaded. The RGB (red-green-blue) quick look view of the image is produced. Quick look view helped to select the data sets that can be used for further processing. Some of the datasets, depending on time of the year, has more cloud coverage. Especially if the region of interest is mostly covered by clouds then it has to be rejected for processing. In Sentinel-2 images with bands of 10 m resolution are preprocessed to decrease to 20 m resolution to have all spectral bands taken to be under consideration for processing having same spatial resolution. Three bands at 60 m resolutions B1, B9 and B10 are not considered for processing as they are mainly used for atmospheric corrections. In case Landsat-8 images band 2, 3, 4, 5 and 6 are considered for processing. All bands are of 30 m

resolution. The datasets are divided into two groups as changed and unchanged group. The unchanged group is used for multivariate probabilistic modelling. First the images in this group are co-registered with respect to the first image. In most of the cases the images from multispectral satellite are ortho-rectified. Even then, the images taken at different instant and from different orbit can cause mis-registration. FFT co-registration approach [8] is used to estimate registration error between the satellite images from the same Sentinel-2 tiles and Landsat- 8 products.

TABLE II
SPATIAL RESOLUTION (M) AND SPECTRAL RANGE (NM) OF LANDSAT-8

Band Number	Spatial Resolution in m	Spectral Range in nm
B1 Coastal/Aerosol	30	435-451
B2 Blue	30	452-512
B3 Green	30	533-590
B4 Red	30	636-673
B5 NIR	30	851-879
B6 SWIR-1	30	1566-1651
B7 SWIR-2	30	2107-2294
B8 Pan	15m	503-676
B10 TIR-1	100	10600-11190
B11 TIR-2	100	11500-12510

III. CHANGE DETECTION METHOD

The pixel based change detection analysis is done using statistical composite hypothesis theory by accumulating multispectral data set over a time of about three years.

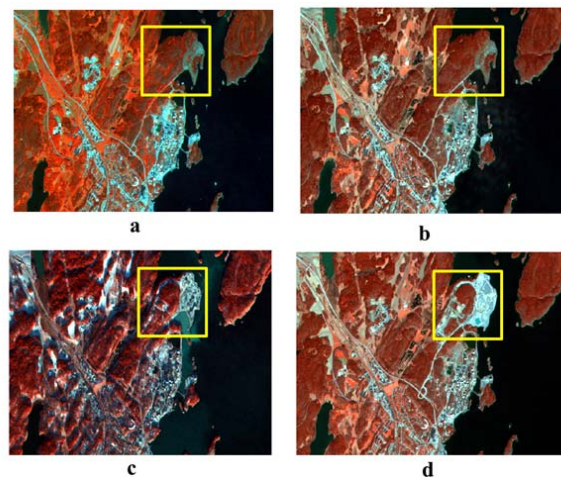


Fig. 2 Color Composite images of the region of interest indicating change occurring over time (a: date 2015-07-04, b: date 2016-05-02, c: date 2016-11-28, d: date 2017-05-04)

The color composite images of band 7-3-2 shown in Fig. 2 are an example showing the conversion of green land to developing built-up area during the time period of 2015 to 2017. Fig. 2 shows that from 2015 June to 2016 May, there is no significant change but the activity started approximately from end of 2016 and the last image shows maximum change in 2017. Fig. 3 shows the comparison of two dimensional covariance plot of Red and NIR (near infra-red) band of same

pixel region at different dates of Sentinel-2 image. The figure explains that the spread along red band is much more in last two dates in 2017. It indicates that change from green vegetation to build-up land.

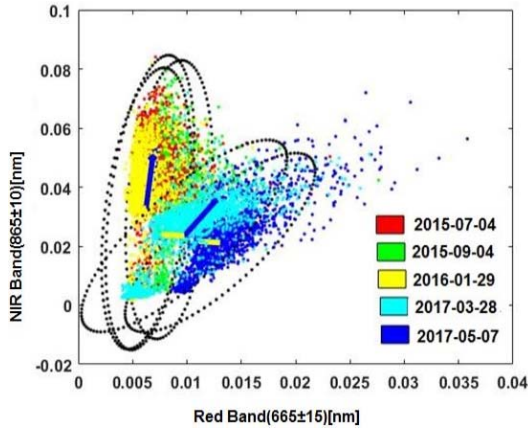


Fig. 3 Comparison of two dimensional covariance plots of same pixel regions but from different dates of Sentinel-2 Image

A. Target Pixel Detection

Statistical composite hypothesis testing is well established technique for target detection from background clutter. This technique is used here to detect the change pixel-wise [9]. Construction of such sets to make a decision of target or a background requires knowledge of a pair of probability density functions (pdfs) defined over some variate, called a feature vector expressed as [9]:

$$p(x) = \frac{1}{(2\pi)^{\frac{d}{2}} |\Sigma|^{\frac{1}{2}}} \exp\left[-\frac{1}{2}(x-\mu)'(x-\mu)\right] \quad (1)$$

where, $p(x)$ is the pixel-wise distribution over time, d the spectral dimensionality, μ is the spectral component mean vector, Σ is $d \times d$ covariance matrix and the determinant is represented as $|\Sigma|$. The composite hypothesis (CH) testing problem is considered [7] here to detect the changed pixel from probabilistic models of the targets and background. The background is modelled as multivariate probability distribution function for a set of same corresponding pixels over time. Likelihood ratio test (LRT) [10] is a discriminant function in the form expressed in (2) to choose the target pixel between two hypothesis H_0 (unchanged pixel) and H_1 (changed pixel):

$$d(x:T, B) \equiv \frac{p_T(x:T)}{p_B(x:B)} - \lambda \quad (2)$$

where $p_T(x:T)$ the probability distribution of target pixels to

be determined as changed or unchanged and $p_B(x:B)$ is the unchanged pixel distribution modelled as background pixels. ' λ ' is an adjustable threshold value depending upon educated guess. CH gets confused when the aim is to distinguish between two families. The clairvoyant solution chooses a single member from each family and then uses the ratio of their likelihoods. In such case, the discriminant test is known as 'clairvoyants' and discriminant detectors are known as clairvoyant detectors. If there is no single target distribution and a single background distribution and rather a set of families of distributions for the target and/or background then the obvious procedure is to parameterize these families with $\theta_T \in \Theta_T$ and $\theta_B \in \Theta_B$ respectively. That is, $p_T(x:\theta_T)$ is the probability distribution of the target and $p_B(x:\theta_B)$ is the probability distribution of the background. GLRT is used due to unknown values of parameters and these parameters are estimated through maximum-likelihood methods (MLE). The discriminant function for the GLRT depends on an educated guess for the values of the threshold parameter. Higher value indicates fewer false alarms, but less probability of target detection, whereas lower threshold gives large false alarm rate. A detection algorithm is defined as a collection of decision rules:

$$d_{GLRT}(x:\lambda) = \frac{\text{Max}_{\theta_T \in \Theta_T} p_T(x:\theta_T)}{\text{Max}_{\theta_B \in \Theta_B} p_B(x:\theta_B)} - \lambda \quad (3)$$

Alternative way of writing the same expression is:

$$d_{GLRT} = \text{Max}_T(\text{Min}_B[d(x:\theta_T, \theta_B, \lambda)]) \quad (4)$$

GLRT is producing a detection algorithm by fusing all the clairvoyant detectors [7]. The *Min* operation generates a discriminant function by fusing all clairvoyants corresponding to different values of background pixels (for a fixed T -values). Similarly, the *Max* operation fuses by forming a critical region that is the union of those of its constituent detectors. Due to registration error changed pixel may not be that corresponding pixel but its neighbor. Therefore in this target pixel is not only the corresponding to background pixel but also 8-neighbourhood pixels. These pixels are taken into account for change detection which can reflect the co-registration accuracy also.

IV. RESULTS AND ANALYSIS

The general procedure of processing frame work for analysis of datasets of Sentinel-2 and Landsat 8 are shown in the form of flow chart in Fig. 5.

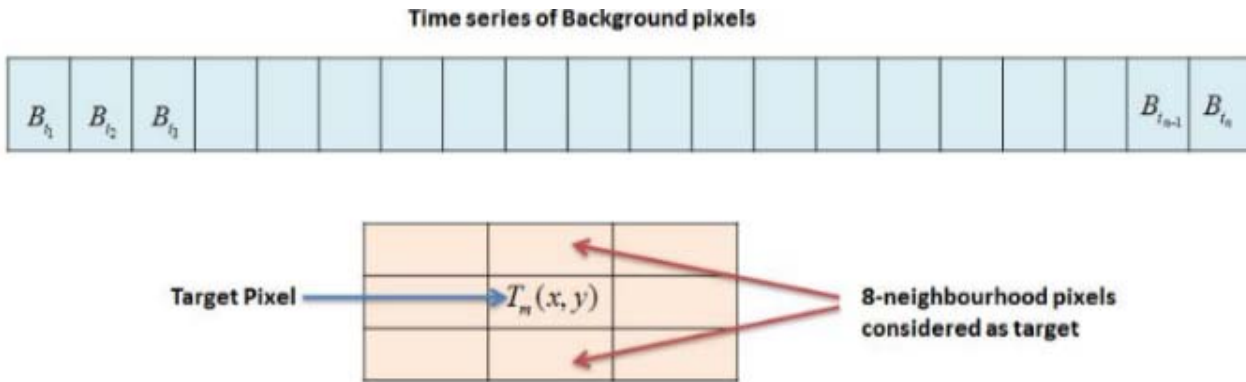


Fig. 4 Time series of background pixels and 8-neighbourhood of target pixels

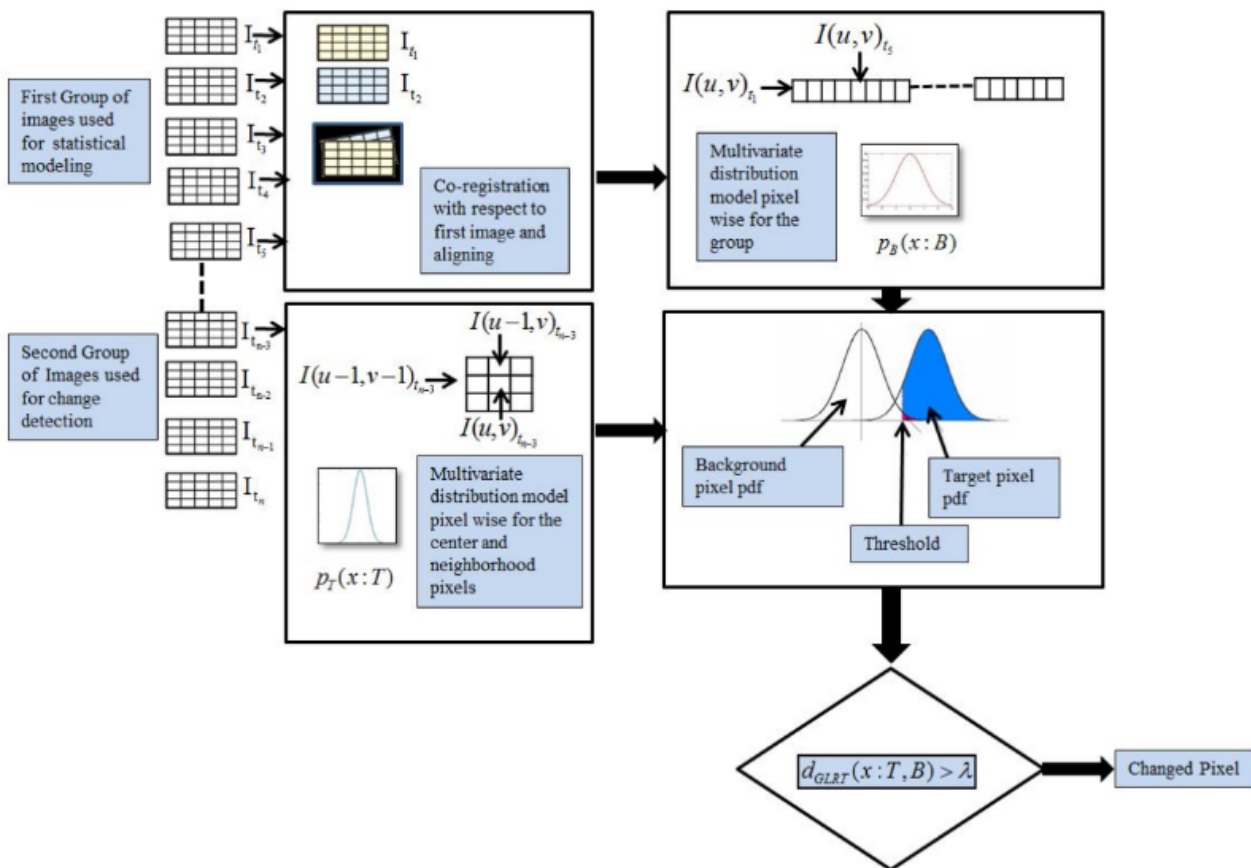


Fig. 5 Processing framework of Sentinel-2 and Landsat-8 images

The comparison of scattered plots in 2015 and 2017 as shown in Fig. 6 indicates the phenomenon of more spread along Red band in later date. It predicts the change in vegetation class to build up class. Fig. 7 shows the result of changed pixels of GLRT test during different months of the year 2017.

Fig. 8 shows an interesting phenomenon. Instead of region of interest, the whole (1000 x 1000) image is processed to estimate the detected changed pixels. This particular image has clouds here and there. The clouds are also detected as

changed pixels along with the changed pixels in the area of interest.

Some examples with detected changed pixels in Landsat-8 images in and around the region of interest during different times of 2017 and 2016 are shown in Fig. 9. The fourth image has a part covered with clouds and it is not at all of good quality for processing. In spite of that, it shows some detected changed pixels over the region of interest selected, shown by red circles. Lastly Fig. 10 is an example of Sentinel-2 and Landsat-8 image at same year and approximately within a gap

of four months. Comparison between them visually shows that some detected changed pixels are nearly over the same area.

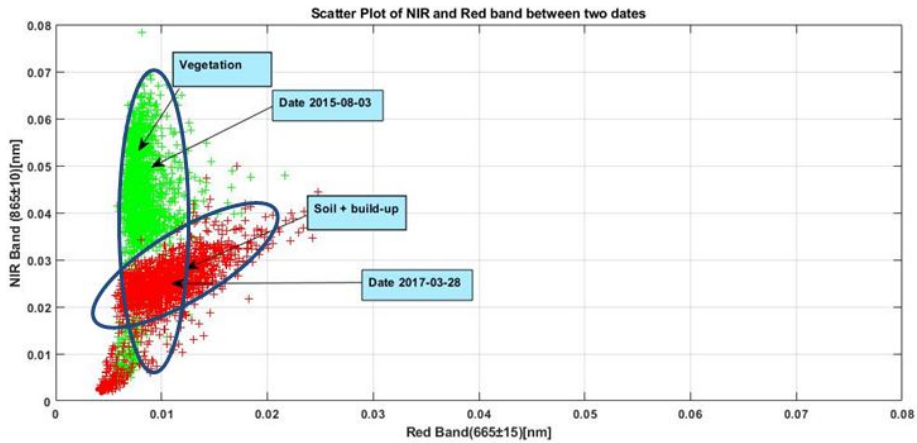


Fig. 6 Scattered plot at same pixel regions but from two different dates from Sentinel-2 images



A rough estimate is done to evaluate the correctness of threshold, varying its value. Fig. 11 shows the variation of changed detected pixels with varying threshold values for Sentinel-2 Dataset taken on 28th March, 2017. The detected pixels in yellow circle region may be false detection for low threshold value, whereas in the region of green circle there is high probability of missed detection due to high value of threshold. So a compromise between 2.33 and 3.09 is set in case of Sentinel-2 Dataset. This is verified for other datasets also.

Fig. 7 The changed pixels shown as red squares in three different dates of Sentinel-2 images as a result of GLRT test

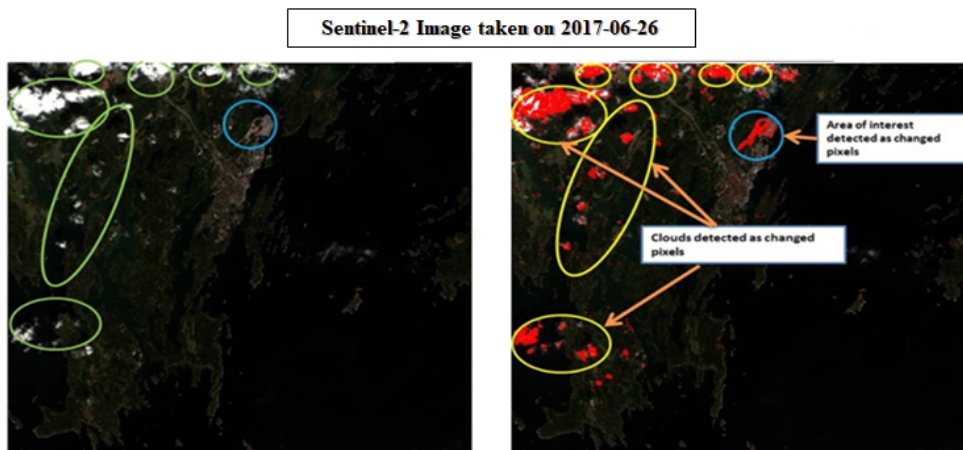


Fig. 8 The specific changed region as well as clouds also showing results of changed pixel

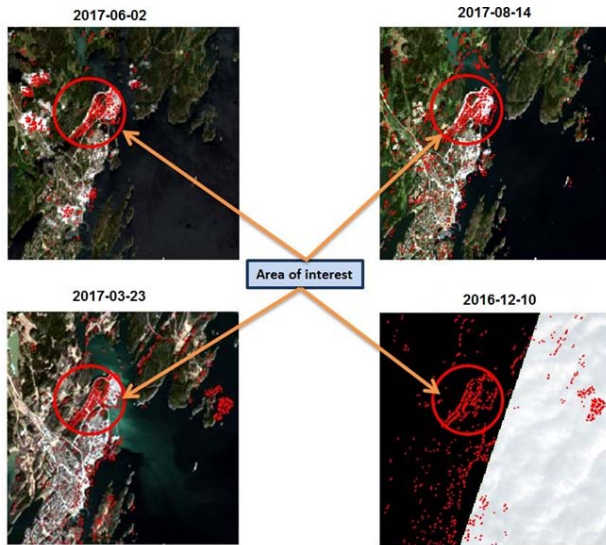


Fig. 9 Lansat-8 images at different dates showing changed pixels
Sentinel Image 2017-07-23 Landsat 8 Image 2017-03-23



Fig. 10 The detected changed pixels shown both in Sentinel-2 and Landsat-8 in approximately four months gap

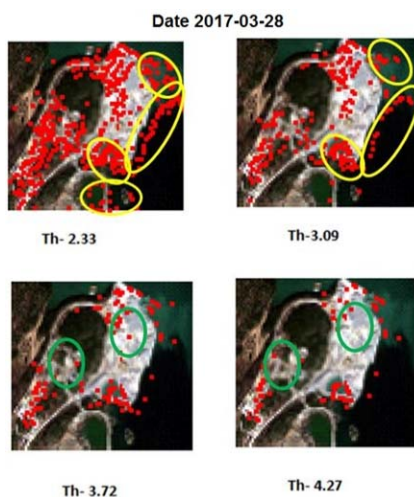


Fig. 11 Sentinel-2 dataset using various threshold values

V.CONCLUSION

There are different challenges in this method. First and foremost challenge is to get quite a large number of datasets for multivariate distribution modelling. The multispectral images acquired are from different time of the year and with

different weather conditions. So a large number of images are always discarded due to cloud coverage. Due to imperfect modelling there will be high probability of false alarm. Co-registration error between the images gives error when the change is detected considering (nominal) corresponding pixels. Therefore 8-neighborhood pixels around the pixel under test are considered. Overall conclusion that can be drawn from this work is that the probabilistic method described in this report has given some promising results, which can be further developed to get more accurate results.

REFERENCES

- [1] S. Kotkar and B. Jadhav, "Analysis of various change detection techniques using satellite images," in 2015 International Conference on Information Processing (ICIP), Pune, India, 2015.
- [2] I. R. Hegazy and M. R. Kaloop, "Monitoring urban growth and land use change detection with GIS and remote sensing techniques in Daqahlia governorate Egypt," *International Journal of Sustainable Built Environment*, vol. 4, no. 1, pp. 117-124, 2015.
- [3] P. Xiao, X. Zhang, D. Wang, M. Yuan, X. Feng and M. Kelly, "Change detection of built-up land: A framework of combining pixel-based detection and object-based recognition," *ISPRS Journal of Photogrammetry and Remote Sensing*, vol. 119, pp. 402-414, 2016.
- [4] S. Aleksandrowicz, S. Lewinski and Z. Bochenek, "Change Detection Algorithm for the Production of Land Cover Change Maps over the European Union Countries," *Remote Sensing*, vol. 6, no. 7, pp. 5976-5994, 2014.
- [5] A. Stumpf, D. Michea and J. P. Malet, "Improved Co-Registration of Sentinel-2 and Landsat-8 Imagery for Earth Surface Motion Measurement," *Remote Sensing*, vol. 10, no. 2, pp. 160-180, 2018.
- [6] D.LU, P. Mausel, E. Brondizio and E. Moran, "Change detection techniques," *International Journal of Remote Sensing*, vol. 25, no. 12, pp. 2365-2407, 2004.
- [7] A. Schaum, "Clairvoyant fusion: a new methodology for designing robust detection algorithms," in *Proc. SPIE 10004, Image and Signal Processing for Remote Sensing XXII*, 18 Oct. 2016.
- [8] M. Guizar-Sicairos, S. T. Thurman and J. R. Fienup, "Efficient subpixel image registration algorithm," *OPTICS LETTERS*, vol. 33, no. 2, pp. 156-158, 2008.
- [9] A. Schaum, "Theoretical foundation of NRL spectral target detection algorithm," *Applied Optics*, vol. 54, no. 31, pp. 288-296, Sept. 2015.
- [10] A. Schaum, "CFAR fusion: A replacement for generalized likelihood ratio test for Neyman-Pearson problems," *IEEE Computer Society*, pp. 1-6, 2011.